Proceedings of the 21st ICSMGE, Vienna, Austria, 14 – 19 June 2026. Pistrol, Adam & Schweiger (eds.)
Published by: ÖGG, Austrian Society for Geomechanics, Salzburg, Austria, ISBN 978-3-9503898-4-5
https://doi.org/10.53243/ICSMGE2026-592

Optimizing CAES Lined Rock Cavern Diameter

Wenbin Fei, Aohui Zhou
College of Civil Engineering, Hunan University, Changsha, Hunan,410082, China

Peng Li
Powerchina Zhongnan Engineering co., LTD., Changsha, Hunan,410014, China

ABSTRACT: In recent years, China has actively promoted renewable energy power stations to achieve carbon peaking and neutrality goals. However, the inherent volatility of renewable energy often leads to mismatches between power generation and consumption peaks, driving a surge in demand for energy storage facilities. Currently, mature large-scale energy storage technologies include pumped hydro storage (PHS) and compressed air energy storage (CAES). Lined rock cavern (LRC), less constrained by geological site selection, has gained attention as an ideal solution for CAES. For LRC using steel for sealing, cost variability primarily depends on the mass and type of steel required. Optimizing cavern dimensions to minimize steel usage while meeting operational requirements is crucial to reducing costs. This study derives a formula for calculating the total steel lining mass for gas storage caverns under specific parameters and proposes a procedure to optimize cavern diameter. The core idea is to optimize the cavern diameter, under the constraint of steel lining thickness (14~50mm) and with all other design parameters given, in order to minimize the total mass of the steel lining. A sensitivity analysis evaluates the effects of factors such as maximum storage pressure (P), stee lining design strength (σ_R). surrounding rock resistance coefficient (K_0), total gap (δ), and cavern radius (R) on steel lining mass. Results show that steel lining mass decreases and then increases with rising storage pressure, decreases with higher design strength, greater rock resistance, or larger cavern radius, but increases with wider construction gaps. These findings emphasize the importance of favorable rock conditions, strict gap control, and carefully designed storage pressure. Additionally, selecting steel balanced between price and strength is vital to minimizing costs in LRC.

KEYWORDS: Compressed air energy storage; Lined rock cavern; Optimal cavern diameter; Steel costs

1 INTRODUCTION

China is actively promoting the deployment of renewable energy power stations to achieve its carbon peaking and carbon neutrality goals (Chen et al., 2022, Wang et al., 2021, Zhao et al., 2022). During the 14th Five-Year Plan period, the nation aims to maintain an annual increase of over 100 GW in newly installed renewable capacity. This expansion is particularly pronounced in regions such as Xinjiang, Gansu, and eastern Inner Mongolia, where renewable power generation has grown rapidly, reaching 1.1, 1.4, and even 2.0 times the maximum local electricity demand. However, the inherent intermittency of renewable energy sources has led to a significant mismatch between electricity generation and consumption peaks, resulting in severe renewable energy curtailment. In extreme cases, curtailment—encompassing wind, solar, and hydro—has reached as much as 102.3 billion kWh per year, surpassing the annual output of the Three Gorges Dam (National-Energy-Administration, 2024b, The-State-Council-of-the-People's-Republic-of-China, 2019). Similar integration challenges and renewable energy curtailment have also been reported internationally as wind and solar penetration increases, underscoring a global need for long-duration, grid-scale storage (Liang et al., 2024, Kebede et al., 2022). Yet, the arid conditions in some regions make them unsuitable for the construction of pumped hydro storage facilities (Beijing-Energy-Concsevation-and-Environment-Protection-Center, 2024). In response, lined rock cavern (LRC)-based compressed air energy storage (CAES) has emerged as a promising solution due to its lower dependence on specific geological formations (Zhou et al., 2025, Jiang et al., 2020). Meanwhile, LRC-CAES offers several other advantages compared with other storage technologies. It utilizes underground space to minimize surface land use, provides long-life infrastructure that lowers lifecycle cost for long-duration storage, and—by thermodynamic design—decouples power and energy for flexible system sizing. As such, LRC-CAES technology holds significant potential for large-scale deployment across China (Xia et al., 2022) and even the all over the world.

In LRC for CAES, aboveground facility costs are relatively fixed, while underground storage costs can vary significantly, often accounting for 50-60% of the total project cost. With the cavern volume fixed under specific power generation and pressure conditions, excavation costs remain stable. For gas storage using steel for sealing, cost variability primarily depends on the mass and type of steel required. Optimizing cavern dimensions to minimize steel usage is crucial for reducing costs. This study proposes a method to optimize cavern radius and conducts a sensitivity analysis to assess the influence of design parameters on the thickness and mass of the steel lining.

2 OPTIMAL CAVERN DIAMETER DETERMINATION METHOD

2.1 *Calculation method*

Under the premise of a fixed power generation capacity, the required cavern volume V_{st} of the LRC can be calculated based on the processes of the compressor and the expander, in conjunction with the properties of the compressed air. The calculation formulas for the area of the circular tunnel section and the cavern volume are as follows:

$$S = \pi R^2 \tag{1}$$

$$V_{st} = SL \tag{2}$$

Among these, R represents the cavern radius (m), L is the cavern length (m), S denotes the cross-sectional area of the cavern (m^2), V_{st} represents the volume of the cavern (m^3).

The structure of the LRC is illustrated in Figure 1. From the inside out, it comprises steel lining, concrete lining, and the surrounding rock. Under high internal pressure, the surrounding rock undergoes plastic deformation, leading to the formation of a plastic deformation gap of surrounding rock, denoted as δ_p. Subjected to cyclic temperature variations, the temperature gradient and the differences in thermal expansion coefficients induce a thermal gap of the steel lining, denoted as δ_s. Additionally, a construction gap, δ_b, is generated during the

construction process. is also occurred. Therefore, the total gap δ within the LRC is the sum of δ_p, δ_s and δ_b.

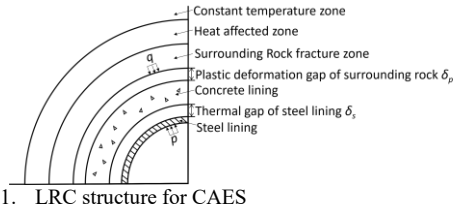

Figure 1. LRC structure for CAES

According to the "Code for design of underground air storage for compressed air energy storage reservoir power station"(National-Energy-Administration, 2024a), the thickness of the steel lining is:

$$t = \frac{P_{max}R}{\sigma_R} + 1000K_0\left(\frac{\delta}{\sigma_R} - \frac{R}{E_{S2}}\right) \quad (3)$$

In the formula, t represents the thickness of the steel lining (mm), P_{max} is the maximum internal pressure in the LRC gas storage (MPa), σ_R is the steel lining design strength (MPa), K_0 is the surrounding rock resistance coefficient (N/mm^3); δ is the total gap (mm), E_{s2} denotes the elastic modulus of steel under planar strain condition (MPa). $\frac{P_{max}R}{\sigma_R}$ is the design thickness of the steel lining when bearing alone. $1000K_0\left(\frac{\delta}{\sigma_R} - \frac{R}{E_{S2}}\right)$ calculates the reduction in the thickness of the steel lining by the load shared by the surrounding rock. Therefore, the steel mass can be calculated as:

$$V_{sl} = 2\pi RLt \quad (4)$$

$$m = \rho V_{sl} \quad (5)$$

Among them, V_{sl} represents the steel volume (m^3), m is the steel mass (kg), ρ is the steel density (kg/m^3). By combining Equations (1) to (5), the following is obtained:

$$m = \frac{2\rho V_{st}P_{max}}{\sigma_R} - \frac{2000K_0\rho V_{st}}{E_{S2}} + \frac{2000K_0\rho V_{st}\delta}{R\sigma_R} \quad (6)$$

According to engineering experience, the minimum steel lining thickness is set at 14 mm. And, when the thickness exceeds 50 mm, construction becomes quite difficult. Therefore, before calculating the steel lining mass, the thickness must first be determined. If the thickness is less than 14 mm, the quality calculation should use 14 mm. If the thickness exceeds 50 mm, a new design plan should be developed. Based on this, Equation (6) is revised as follows:

$$m = 0.001\left(\frac{2\rho V_{st}P_{max}}{\sigma_R} - \frac{2000K_0\rho V_{st}}{E_{S2}} + \frac{2000K_0\rho V_{st}\delta}{R\sigma_R}\right) \quad 14 < t \le 50 \quad (7)$$

$$m = \frac{0.028\rho V_{st}}{R} \quad t \le 14$$

It can be seen from Equation (7) that for the case where the steel lining thickness is between 14mm and 50mm, and when design parameters are fixed, the first two terms of the formula are constant values, while the size of the third term is inversely proportional to the cavern radius. For cases where the thickness is less than 14mm, the steel mass is also inversely proportional to the cavern radius. Therefore, the process shown in Figure 2 can be used to find the optimal radius to minimize the mass of the steel lining: ① Determine the design parameters and the maximum radius R_1 under the surrounding rock conditions of the project; ② Substitute the design parameters into Equation (3) to obtain the maximum radius R_2 when the steel lining thickness is equal to 14mm and the maximum radius R_3 when the thickness of the steel lining thickness is equal to 50mm respectively; ③ Compare the values of R_1, R_2 and R_3. If $R_1 > R_3 > R_2$, substitute R_3 into the first expression of Equation (7) to calculate m_1, and substitute R_2 into the second expression of Equation (7) to calculate m_2. The radius corresponding to the smaller value in m_1 and m_2 is the optimal radius. If $R_3 > R_1 > R_2$, then substitute R_1 into the first expression of Equation (7) to calculate m_1, and substitute R_2 into the second expression of Equation (7) to calculate m_2. The radius corresponding to the smaller values in m_1 and m_2 is the optimal radius. If $R_3 > R_2 > R_1$, then R_1 is the optimal radius.

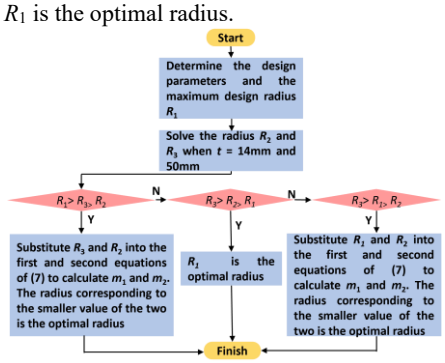

Figure 2. Process for determining the optimal cavern diameter

2.2 *Calculation examples*

2.2.1 *Example 1*

The maximum pressure P is taken as 12 MPa, which corresponds to a storage cavern volume V_{st} of 215,690.7 m^3. The type of steel lining is 07MnMoVR, with a design strength σ_R of 304 MPa. The surrounding rock resistance coefficient K_0 is set to 8.4 N/mm^3, and total gap δ is 0.2mm. The density of the steel lining ρ is 7850 kg/m^3. The elastic modulus of steel under planar strain condition E_{s2} is 226373.63MPa. The maximum design radius R_1 is 8000mm. Substituting these parameters into Equation (3) yields:

$$t = 0.002367R + 5.5263 \quad (8)$$

Figure 3 illustrates the relationship between the steel lining thickness and the cavern radius under the given design parameters. It can be observed that when the cavern radius is smaller than 3,580 mm, the steel lining thickness will be less than 14 mm. Conversely, when the radius exceeds 18,789 mm, the steel lining thickness will exceed 50 mm. Therefore, for this scenario, R_1 = 8000 mm, R_2 = 3580 mm, and R_3=18789 mm, where $R_3 > R_1 > R_2$. This satisfies the third case in the calculation process. Substituting R_1 = 8000 mm into the first equation of Equation (7) and R_2 = 3580 mm into the second equation of Equation (7) yields:

$$m_1 = 10354 \quad (9)$$

$$m_2 = 13242 \quad (10)$$

Therefore, the optimal radius for this example is 8,000 mm.

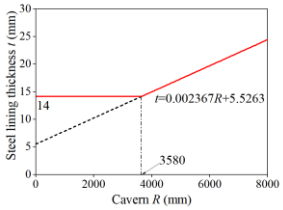

Figure 3. Relationship between R and t (K_0 = 8.4N/mm^3)

2.2.2 *Example 2*

The surrounding rock resistance coefficient K_0 is set to 7.2N/mm^3, with all other parameters remaining the same as in Example 1. Substituting these parameters into Equation (3) yields:

$$t = 0.007668R + 4.7368 \quad (11)$$

Figures 4 illustrate the relationship between the steel lining thickness and the cavern radius under this design scenario. It can be observed that when the cavern radius is smaller than

1,208 mm, the steel lining thickness will be less than 14 mm. Conversely, when the radius exceeds 5,902 mm, the steel lining thickness will exceed 50 mm. Therefore, in this scenario, R_1=8000 mm, R_2=1208 mm, R_3=5902 mm, where $R_1 > R_3 > R_2$.This satisfies the first case in the calculation process. Substituting R_3=5902 mm into the first equation of Equation (7) and R_2=1208 mm into the second equation of Equation (7) yield:

$$m_1 = 28683 \quad (12)$$

$$m_2 = 39245 \quad (13)$$

Therefore, the optimal radius for this example is 5,902 mm.

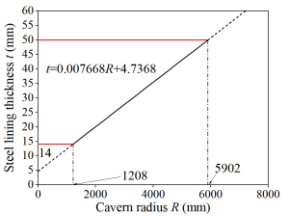

Figure 4. Relationship between R and t (K_0 = 7.2N/mm^3)

3 PARAMETER ANALYSIS AND DISCUSSION

It can be found that the main factors determining steel lining mass are P (affects V_{st}, relationship between P and V_{st} can be seen in Table1), σ_R, K_0, δ and R.To analyze the sensitivity of the steel mass to the above factors, the parameters given in Table 2 were used for calculation. When studying the effect of a single parameter, the other parameters were held constant.

Table 1. Relationship between P and V_{st}

P (MPa)	10	11	12	13
V_{st} (m^3)	235710.8	224160.9	215690.7	209116.1
P (MPa)	14	15	16	17
V_{st} (m^3)	203807.9	199396.5	195648.4	192407.8
P (MPa)	18	19	20	
V_{st} (m^3)	189566.0	187044.9	184786.2	

Table 2. Calculation parameter

Parameter	Value	Parameter	Value
P	11MPa	δ	0.2mm
V_{st}	224160.9m^3	R	6000mm
σ_R	304MPa	ρ	7850kg/m^3
K_0	7N/mm^3	E_{S2}	226373.63MPa

3.1 *Effect of P* (V_{st})

Figure 5 illustrates the variation of steel lining thickness and total mass with respect to the maximum design pressure P. When P ranges between 10 and 12 MPa, the computed steel liner thickness remains below 14 mm; therefore, a structural thickness of 14 mm is adopted. As P continues to increase beyond this range, the thickness exhibits a sharp linear escalation, surpassing 50 mm when P reaches 15 MPa. When the lining thickness is fixed at 14 mm, a slight decrease in the total steel mass is observed with increasing P. However, once the thickness exceeds 14 mm, the total mass increases rapidly and approximately linearly with P increasing. Specifically, for every 1 MPa increment in P, the lining thickness increases by an average of 20 mm, resulting in an additional 9,278.3 t of steel. Overall, the total mass of the steel lining initially decreases and then increases as P rises. It is worth noting, however, that if the required lining thickness already exceeds 14 mm under other design conditions at P=10 MPa, the total mass will increase linearly and rapidly with further increases with P increasing.

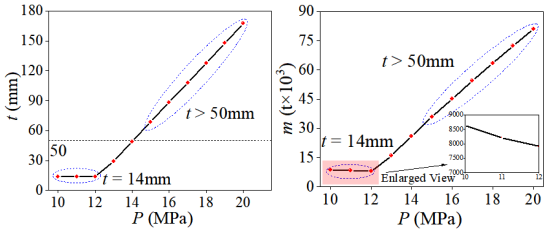

Figure 5. Thickness and mass of the steel lining evolve with P

3.2 *Effect of* σ_R

For safety considerations, the design strength σ_R of the steel liner is typically taken as 60%–70% of the yield strength of the steel. A parametric sensitivity analysis was conducted using commonly employed high-pressure vessel steels—Q345, Q490, Q550, Q620, and Q690—with corresponding σ_R of 232 MPa, 304 MPa, 358 MPa, 403 MPa, and 450 MPa, respectively.

Figure 6 presents the variation of steel lining thickness and total mass with respect to σ_R. For Q345 and Q490, increases in σ_R result in a marked reduction in both lining thickness and mass. However, when using Q345, the required lining thickness exceeds 50 mm. In contrast, for higher-strength steels such as Q550, Q620, and Q690, the calculated lining thickness remains below 14 mm, and thus a minimum structural thickness of 14mm is adopted in all cases, resulting in identical steel mass requirements. Generally, higher-strength steels tend to be more expensive. Therefore, material selection should balance both mechanical performance and economic considerations. Based on the trade-off between required thickness and material cost, Q490 is recommended as a suitable choice for the steel lining.

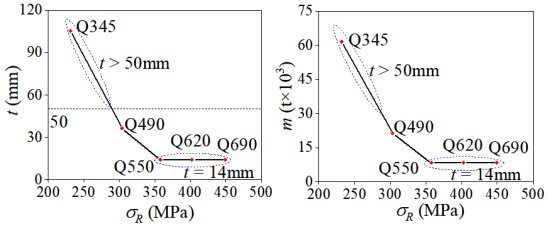

Figure 6. Thickness and mass of the steel lining evolve with σ_R

3.3 *Effect of* K_0

Higher rock mass grade corresponds to greater resistance coefficient K_0. In general, for CAES caverns, the surrounding rock should be at least Grade II, which typically corresponds to K_0>5 N/mm^3.

Figure 7 depicts the evolution of steel lining thickness and total mass as functions of K_0. When K_0 is less than 8 N/mm^3, the lining thickness decreases approximately linearly with increasing K_0. Once K_0 exceeds 8 N/mm^3, the required lining thickness reaches the structural minimum of 14 mm. In scenarios where the lining thickness exceeds 14 mm, a further decrease in K_0 leads to a rapid linear increase in total steel mass. Specifically, for every 0.2 N/mm^3 reduction in K_0, the lining thickness increases by an average of 5.2 mm, and the total steel mass increases by approximately 3,032.1 t. These findings underscore the critical importance of site selection for CAES cavern. Locating caverns in regions with competent rock masses can substantially reduce steel lining mass.

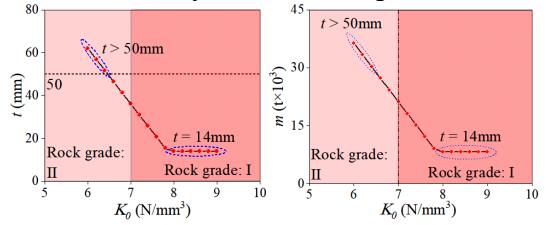

Figure 7. Thickness and mass of the steel lining evolve with K_0

3.4 *Effect of δ*

In LRC, three types of gaps are typically present within the lining structure: construction gap, thermal gap, and plastic deformation gap. Under ideal construction conditions, the total gap δ can be minimized to approximately 0.2 mm. A parametric sensitivity analysis was conducted for δ of 0.2 mm, 0.3 mm, 0.4 mm, 0.5 mm, and 0.6 mm.

Figure 8 illustrates the variation in steel lining thickness and total mass with respect to changes in δ. Both lining thickness and total steel mass increase linearly with the widening of δ. Specifically, for every 0.1 mm increase in δ, the lining thickness rises by approximately 2.3 mm, while the total steel mass increases by around 1,350 t. These results highlight the necessity of strict control gap formation during construction. Minimizing δ is essential to reducing steel lining thickness and material usage.

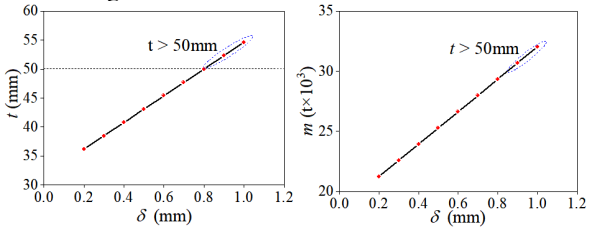

Figure 8. Thickness and mass of the steel lining evolve with δ

3.5 *Effect of R*

The cavern radius R is governed by a combination of factors, including the required gas storage volume, cavern burial depth, and the stability of the surrounding rock mass. A parametric sensitivity analysis was performed for R of 4000 mm, 4500 mm, 5000 mm, 5500 mm, 6000 mm, 6500 mm, 7000 mm, 7500 mm, and 8000 mm.

Figure 9 presents the evolution of steel lining thickness and total mass as functions of R. The lining thickness increases approximately linearly with R; for every 0.5 m increase in R, the required lining thickness rises by about 2.6 mm. Conversely, the total steel mass exhibits an inverse relationship with R: larger R are associated with reduced steel consumption.

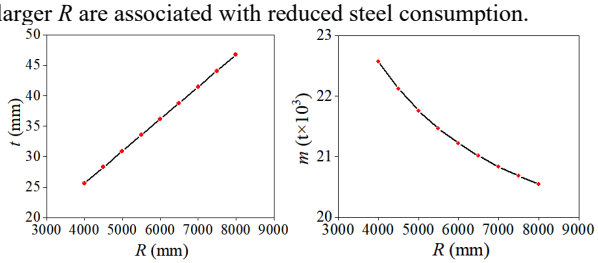

Figure 9. Thickness and mass of the steel lining evolve with R

3.6 *Discussion*

From the perspective of the project workflow—site selection, design, and construction—the parameter influences can be summarized concisely as follows. At the site-selection stage, a higher rock resistance coefficient K_0 directly lowers the required steel mass. So, selecting a geologically favorable site is the most effective measure. At the design stage, the cavern radius R and maximum design pressure P should be chosen judiciously: for a fixed storage volume, increasing R shortens the length and can reduce total steel mass, but the upper bound of R is constrained by span stability limits; P should meet storage needs without unnecessarily increasing steel. The steel design strength σ_R can reduce thickness, yet the benefit plateaus once the minimum thickness governs, so a reasonable grade is preferred over simply pursuing higher strength. At the construction stage, improving construction quality to control the total gap δ can reduce steel consumption.

Notably, this study focuses solely on the steel lining mass as an indicator for optimizing the cavern radius. In the future, the costs associated with support, underground equipment, and other factors will be considered to further optimize the selection of the cavern radius of LRC for CAES.

4 CONCLUSION

This study proposes a method for determining the optimal radius of LRC for CAES, aiming to minimize the weight of the steel lining. Given that other design parameters are fixed, this method can be applied to determine the optimal cavern radius. Additionally, the influence of each design parameter on the mass of steel linings is analyzed.

5 ACKNOWLEDGEMENTS

Thanks to the support of "the R&D project of key technologies of large-scale compressed air energy storage" of Powerchina Zhongnan Engineering co., LTD.

6 REFERENCES

BEIJING-ENERGY-CONCSEVATION-AND-ENVIRONMENT-PROTECTION-CENTER. 2024. *Notice on the Publicity of Typical Cases of Green and Low-Carbon Technologies in Beijing-Tianjin-Hebei Region (2023-2024)* [Online]. [Accessed].

CHEN, R., SU, G. H. & ZHANG, K. 2022. Analysis on the high-quality development of nuclear energy under the goal of peaking carbon emissions and achieving carbon neutrality. *Carbon Neutrality,* 1.

JIANG, Z., LI, P., TANG, D., ZHAO, H. & LI, Y. 2020. Experimental and Numerical Investigations of Small-Scale Lined Rock Cavern at Shallow Depth for Compressed Air Energy Storage. *Rock Mechanics and Rock Engineering,* 53**,** 2671-2683.

KEBEDE, A. A., KALOGIANNIS, T., VAN MIERLO, J. & BERECIBAR, M. 2022. A comprehensive review of stationary energy storage devices for large scale renewable energy sources grid integration. *Renewable and Sustainable Energy Reviews,* 159.

LIANG, Y., LI, P., XING, L., SU, W., LI, W. & XU, W. 2024. Current status of thermodynamic electricity storage: Principle, structure, storage device and demonstration. *Journal of Energy Storage,* 80.

NATIONAL-ENERGY-ADMINISTRATION 2024a. Code for design of underground air storage for compressed air energy storage reservoir power stations.

NATIONAL-ENERGY-ADMINISTRATION. 2024b. *Support Chinese-style modernization with energy transformation and development* [Online]. [Accessed].

THE-STATE-COUNCIL-OF-THE-PEOPLE'S-REPUBLIC-OF-CHINA. 2019. *Strive to basically solve the problem of abandoning water, wind and light by 2020* [Online]. [Accessed].

WANG, Y., GUO, C.-H., DU, C., CHEN, X.-J., JIA, L.-Q., GUO, X.-N., CHEN, R.-S., ZHANG, M.-S., CHEN, Z.-Y. & WANG, H.-D. 2021. Carbon peak and carbon neutrality in China: Goals, implementation path, and prospects. *China Geology,* 4**,** 1-27.

XIA, T., LI, Y., ZHANG, N. & KANG, C. 2022. Role of compressed air energy storage in urban integrated energy systems with increasing wind penetration. *Renewable and Sustainable Energy Reviews,* 160.

ZHAO, C., JU, S., XUE, Y., REN, T., JI, Y. & CHEN, X. 2022. China's energy transitions for carbon neutrality: challenges and opportunities. *Carbon Neutrality,* 1.

ZHOU, A., LI, P., FAN, L., YI, Z., TANG, X. & FEI, W. 2025. Influence of drainage system on the stability of underground CAES gas storage under different lateral pressure coefficients. *Tunnelling and Underground Space Technology,* 159.